Biosensors and Bioelectronics 78 (2016) 483–488

Contents lists available at ScienceDirect

Biosensors and Bioelectronics

journal homepage: www.elsevier.com/locate/bios

Electrochemical biosensor for *Mycobacterium tuberculosis* DNA detection based on gold nanotubes array electrode platform

Sri Ramulu Torati [a], Venu Reddy [a,b], Seok Soo Yoon [c], CheolGi Kim [a,*]

[a] Department of Emerging Materials Science, DGIST, Daegu 711-873, Republic of Korea
[b] School of Engineering Science and Technology, University of Hyderabad, Gachibowli, Hyderabad 500046, India
[c] Department of Physics, Andong National University, Andong 760-749, Korea

ARTICLE INFO

Article history:
Received 2 October 2015
Received in revised form
22 November 2015
Accepted 30 November 2015
Available online 2 December 2015

Keywords:
Electrodeposition
Nanotubes
DNA biosensor
Methylene blue
Hybridization

ABSTRACT

The template assisted electrochemical deposition technique was used for the synthesis of gold nanotubes array (AuNTsA). The morphological structure of the synthesized AuNTsA was observed by scanning electron microscopy and found that the individual nanotubes are around 1.5 μm in length with a diameter of 200 nm. Nanotubes are vertically aligned to the Au thick film, which is formed during the synthesis process of nanotubes. The electrochemical performance of the AuNTsA was compared with the bare Au electrode and found that AuNTsA has better electron transfer surface than bare Au electrode which is due to the high surface area. Hence, the AuNTsA was used as an electrode for the fabrication of DNA hybridization biosensor for detection of *Mycobacterium Tuberculosis* DNA. The DNA hybridization biosensor constructed by AuNTsA electrode was characterized by cyclic voltammetry technique with Fe $(CN)_6^{3-/4-}$ as an electrochemical redox indicator. The selectivity of the fabricated biosensor was illustrated by hybridization with complementary DNA and non-complementary DNA with probe DNA immobilized AuNTsA electrode using methylene blue as a hybridization indicator. The developed electrochemical DNA biosensor shows good linear range of complementary DNA concentration from 0.01 ng/μL to 100 ng/μL with high detection limit.

1. Introduction

Tuberculosis (TB) is common infectious disease caused by the bacillus *Mycobacterium tuberculosis* which usually affects the lungs, and remains the second leading cause of death from an infectious disease worldwide, after the human immunodeficiency virus (WHO Global Tuberculosis Report, 2014). The standard method used for diagnosing of TB is sputum smear microscopy, in which bacteria are examined in sputum samples under a microscope but this method is unable to identify half of the positive TB infections (Chavolla and Alocilja, 2011). Beside this method, various conventional diagnostic methods for TB are recently developed including polymerase chain reaction, immunoassays and southern hybridization (Prabhakar et al., 2008). Even though, these diagnostic methods have high specificity and sensitivity but are known for their limitations in terms of expensive, time consuming, and usage of hazardous materials (Das et al., 2010). Thus, there is a need for a sensitive and cost-effective technique for the diagnosis of TB.

Recent advances in the development of electrochemical DNA biosensors based on nanomaterials have attracted substantial attention towards the potential application of medical diagnosis, gene analysis, food safety and environmental monitoring (Chavolla and Alocilja, 2011; Cai et al., 2003; Kara et al., 2009; Chiti et al., 2001; Abdalhai et al., 2014). Among different nanomaterials, vertically aligned array types of nanostructures are more interesting for the fabrication of biosensors due to high surface area than its counter flat electrode (Bai et al., 2008; Chang et al., 2007; Lin et al., 2004; Wang et al., 2012; Gasparac et al., 2004). The integration of these nanostructures into sensing device, especially in electrochemical devices where the sensitivity depends on the active surface area of the electrode will greatly enhance the sensitivity of the device (Anandan et al., 2006; Hrdy et al., 2013; Szunerits et al., 2015). The high active surface area of the nanostructures will provide high amount of immobilization of probe molecules in biosensors and thus leading to increase the sensitivity (Li et al., 2011; Du et al., 2009; Hill et al., 2009; Fu et al., 2005, Lee et al., 2008). Because of exceptional biocompatibility and chemical stability of gold materials (Shukla et al., 2005; Lee et al., 2014; Wang et al., 2015; Devi et al., 2015), the vertically aligned gold nanotubes array nanostructures could be a good candidate for the electrode

* Corresponding author.
E-mail address: cgkim@dgist.ac.kr (C. Kim).

http://dx.doi.org/10.1016/j.bios.2015.11.098
0956-5663/

of electrochemical DNA biosensors.

The selection of fabrication technique is main issue for the well aligned array types of nanotube/nanowires structures because the size, shape, orientation and crystallinity of the nanotubes are depends on the synthesis technique (Soundararajan et al., 2009; Tang et al., 2008; Yuzvinsky et al., 2006). There are several techniques are available for the fabrication of array type nanostructures such as Physical vapor deposition (PVD), Chemical vapor deposition (CVD) and template assisted electrochemical deposition (Yang et al., 2011; Hong et al., 2010; Yang et al. 2012; Lei et al., 2013). Among these techniques, electrochemical technique is the more suitable because of its potential advantages such as simple, controllable size and cost-effectiveness (Lu et al., 2009; Naderi et al. 2012; Ramulu et al. 2013).

The main concern of fabricating the nanotubes array by PVD and CVD is deformation or bunching of nanotubes array which is due to the large capillary forces generated by the nanostructures-liquid interaction in liquid medium, and such a deformation or bunching of vertically aligned nanostructures will decrease the level of increase in the active surface area (Anandan et al., 2006; Fan et al., 2004, Kralchevsky and Nagayama, 2000). Hence, the above said two techniques for the fabrication of nanotubes array is not suitable for electrochemical biosensors because electrochemical biosensors are usually performed in liquid medium. Therefore, to overcome the above said difficulties, there is a need of good mechanically strength nanostructures which are strongly attach to the substrate and overcome the capillary forces in liquid medium. These nanostructures could be possible through electrochemical deposition technique. Anandan et al. (2006) have fabricated vertically well aligned gold and silver nanopillars array by electrodeposition technique and tested the mechanical strength of nanostructures for electrochemical performance and proved that the nanostructures fabricated by this method are good for electrochemical performance in liquid medium. Yang et al. (2006) have grown highly regular, uniform and vertically oriented platinum nanowire arrays by electrodeposition in polycarbonate membrane for the fabrication of glucose biosensor. Even though, few groups have succeed to synthesis array types nanowire by electrodeposition method, still complexity remains for the fabrication of well aligned nanotubes array because the nanotubes are more delicate and easily can be broken. Hence, we tried to synthesize well aligned nanotubes array for biosensor application by some modification in the synthesis procedure of the electrodeposition technique.

In this article, we have developed a DNA hybridization biosensor for detection of *M. tuberculosis* DNA based on vertically aligned gold nanotubes array (AuNTsA), which was fabricated by electrochemical deposition technique. The electrochemical performance of AuNTsA electrode was tested and also compared with bare Au gold electrode by cyclic voltammetry and found that AuNTsA electrode surface has better electron transfer than bare Au electrode. Hence, the AuNTsA electrode was used for the immobilization and hybridization of DNA. A series of complementary DNA concentration was tested for the evaluation of the detection limit.

2. Experimental details

2.1. Materials and chemicals

A commercially available track-etched polycarbonate (PC) membrane with 200 nm diameter was purchased from Whatman Company. The gold plating solution for the electrodeposition of nanotubes was procured from SME, Korea. Potassium ferricyanide [$K_3Fe(CN)_6$], potassium ferrocyanide [$K_4Fe(CN)_6$], and Tris-EDTA buffer (pH 8) was obtained from Sigma Aldrich. All other chemicals were of analytical grade and used without any further purification. A 0.05 M phosphate buffer saline (PBS) solution was prepared using Na_2HPO_4 and NaH_2PO_4 with 0.9% of NaCl and adjusted to pH 7.4. The deionized water obtained from a Milli-Q water purification system was used throughout the experiments.

The base sequences specified to *M. tuberculosis* (Das et al., 2010) used in the present studies is purchased from GeneChem Inc., Korea and the sequences are given as follows:

(i) *Probe DNA*: 5′-GGT CTT CGT GGC CGG CGT TCA-3′
(ii) *Complementary DNA*: 5′-TGA ACG CCG GCC ACGAAG ACC-3′
(iii) *Non-complementary DNA*: 5′-ATGTCTCAAGCCAGCTGCTG-3′

2.2. Instruments

Electrochemical measurements were performed on an AutoLab (EchoChemie, Netherlands) electrochemical system governed by the GPES software. A conventional three electrode system was used an AuNTsA electrode as working electrode, an Ag/AgCl reference electrode and a platinum sheet counter electrode. The synthesis of AuNTsA was carried out using an electrochemical deposition system (SP-150, BioLogic, France). Scanning electron microscopy (SEM) images were obtained at an operating voltage of 2 kV with Field emission scanning electron microscope (FE-SEM, Magellan400, FEI Company).

2.3. Electrodeposition of nanotubes

The AuNTsA were fabricated by electrodeposition technique using a PC membrane with a pore diameter of 200 nm. The schematic representation of electrochemical synthesis of AuNTsA was shown in Fig. 1. Initially, one side of the PC membrane was sputtered with metallic Au for electric conduction, which served as the working electrode. The details of the electrodeposition of AuNTsA were described elsewhere (Ramulu et al., 2013). In briefly, we started the electrodeposition from gold sputtered side of the membrane by applying −1.0 V. During the deposition process the electrodeposition was taking place bilaterally, that is, both through the pores forming nanotubes and on the exterior of the PC membrane making thicker thin film. This thick film will be well support to the nanotubes for aligning vertically.

The AuNTsA embedded in a PC membrane is then placed on the gold coated glass substrate by conducting paste. Then rubber O-ring was used for proper adjustment of the electrochemical cell on the AuNTsA attached substrate and tightened through metallic clips. After that, dichloromethane was used for the removal PC membrane followed by several times washings with distilled water and allowing for air dry in ordered to get the resultant electrode. These electrodes are used as a working electrode for electrochemical measurements.

2.4. DNA immobilization and hybridization

The AuNTsA electrodes were used to fabricate the DNA biosensor as shown in Fig. 1(b). Immobilization of probe DNA on AuNTsA electrode was achieved by dropping 10 μL of 100 ng/μL probe DNA solution in Tris-EDTA buffer on the surface of the electrodes for 12 h. Then, the electrode was rinsed with Tris-EDTA buffer to remove any non-specifically adsorbed molecules. The hybridization process was performed by dropping 10 μL of different concentration of complementary DNA onto the probe immobilized electrode surface and incubated at 37 °C for 45 min. After hybridization, the bioelectrodes were rinsed with Tris-EDTA buffer and stored at 4 °C when it is not in use.

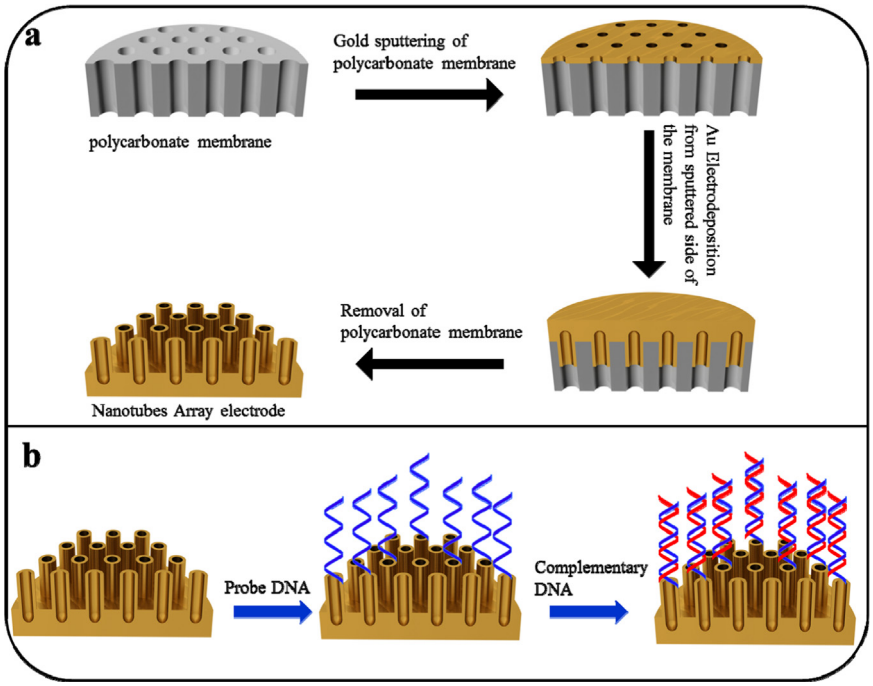

Fig. 1. Schematic drawing of (a) Synthesis of AuNTsA and (b) fabrication of the DNA hybridization biosensor based on AuNTsAelectrodes. (WE – working electrode, RE – reference electrode, CE – counter electrode).

2.5. Electrochemical measurements

The (cyclic voltammetry) CV measurements were performed in a 5 mM $K_3Fe(CN)_6/K_4Fe(CN)_6$ mixtures in 0.05 M PBS solution (pH 7.4). The CV was carried out by varying the scan rate from 10 to 100 mV s^{-1} in a potential range of 0.6 to −0.4 V. The specific hybridization process was monitored via DPV by scanning the potential range of −0.4 to +0.1 in a blank solution of 0.05 M PBS. The bioelectrodes were immersed in 20 μM methylene blue solution in PBS for 5 min before the DPV measurements.

3. Results and discussion

3.1. Characterization of AuNTsA

The structural morphology of the nanotubes was examined by FE-SEM. Fig. 2a and b shows the SEM images of vertically aligned nanotubes. The average length and diameter are found to be 1.5 μm and 0.2 μm, respectively. It can be clear from images that the nanotubes are well vertically aligned and strongly attached to the surface of the Au thick film. The nanotubes are very strong and do not affected by the surface tension of the chemical solvent, dichloromethane which is used for the removal of the template. Moreover, the nanotubes are quite well separated by each other which give good advantages for the electrochemical sensing because each nanotube can acts as an individual nanoelectrode. Inset of Fig.2b shows the single nanotube.

3.2. DNA immobilization and hybridization studies

Fig. 3 shows the cyclic voltammograms obtained for AuNTsA electrode (i) bare Au electrode (ii) thiolated probe DNA immobilized on the AuNTsA electrode (iii) AuNTsA/Probe-DNA/complementary-DNA electrode (iv) in PBS (pH 7.4) containing 5 mM $[Fe(CN)_6^{3-/4-}]$ at the scan rate of 30 mV s^{-1}. A pair of well-defined redox peaks was observed on the bare Au electrode in the potential range of 0.6 to −0.4 V with an anodic peak current (I_a) of 0. 88 mA (curve ii). These peaks are accredited to the redox behavior of $[Fe(CN)_6]^{3-/4-}$ at electrode surfaces. Nevertheless, the AuNTsA electrode have increased peak current, I_a of 1.05 mA (curve i), indicating a better redox behaviors of the redox probe on the AuNTsA electrode. The large surface area of the three-dimensional nanotubes array which increases the active surface area than bare Au electrode may be the reason for increment of I_a of the AuNTsA electrode in comparison with the bare Au electrode (Wang

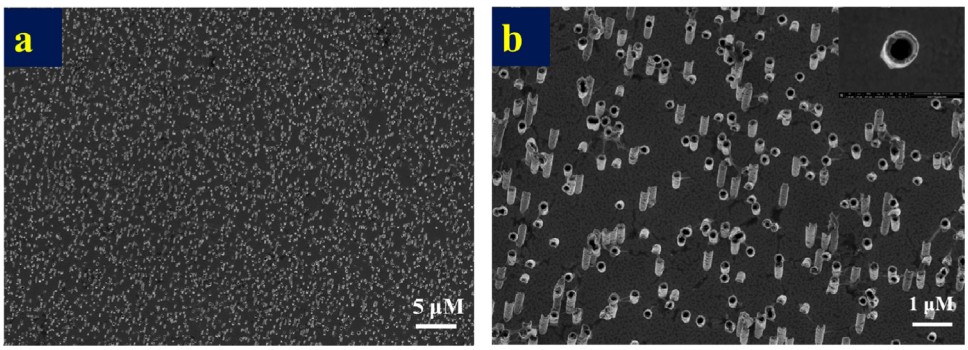

Fig. 2. FE-SEM images of the AuNTsA (a) Low magnification (b) High magnification. Inset shows the single nanotube.

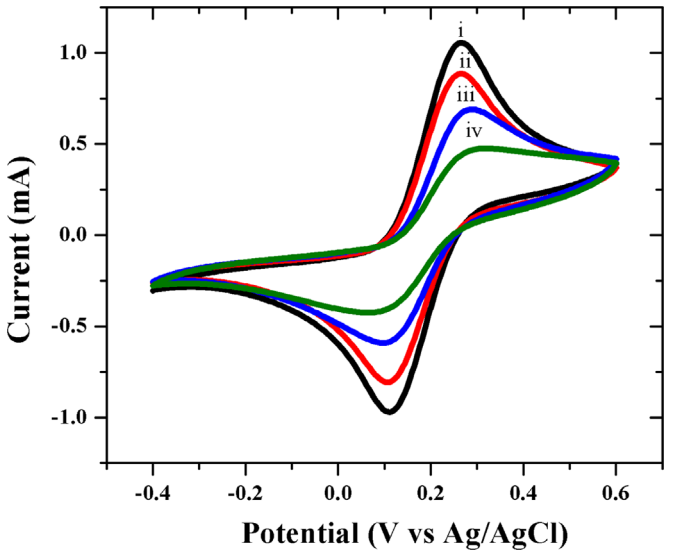

Fig. 3. Cyclic voltagrams of AuNTsA electrode (i) bare Au electrode (ii) AuNTsA/Probe DNA electrode (iii) AuNTsA/Probe/Complementary DNA electrode (iv) in 0.05 M PBS (pH 7.4, 0.15 M NaCl) containing 5 mM $[Fe(CN)_6]^{3-/4-}$.

et al., 2009, 2005). In addition, the AuNTsA electrode opens the possibility of radial diffusion of ions, where as in case of bare Au electrode the only linear diffusion may occurs (Lin et al., 2008). The overall explanation reveals that AuNTsA electrode is more advantageous than the bare Au electrode for the fabrication of electrochemical biosensors. Loading of high amount of probe DNA on the AuNTsA electrode is possible due to its high surface area and obviously it could have better resolution than the bare Au electrode biosensor.

However, after probe DNA immobilization on the AuNTsA electrode, the I_a is decreased to 0.68 mA (curve iii). This could be easily assigned by the limited diffusion of the redox probe toward the electrode surface of the negative charged phosphate backbone of probe DNA (Zheng et al., 2014). This indicates that the probe DNA was successfully immobilized on the AuNTsA electrode surface. When the complementary DNA was hybridized with probe DNA immobilized AuNTsA electrode, there is a further decrease in I_a values (0.50 mA) (curve iv). This could be well explained by the fact that the introduction of complementary DNA increases the negative charge of the phosphate backbone of the DNA, which is responsible for the increased repellence of redox species on electrode surface. The overall explanation indicates that the complementary DNA was successfully hybridized on the probe DNA immobilized on AuNTsA electrode.

The CVs for probe DNA immobilized AuNTsA electrode was investigated by varying the scan rate from 10 to 100 mV/s. It could be seen that when measuring the CVs towards higher scans, there is a shift of the anodic potential towards positive direction and cathodic potential shifts in the reverse trend with an increase of I_a and decrease of I_c respectively (Fig. 4a). The peak currents show a good linear relationship with square root of scan rates (Fig. 4b), indicating a typical diffusion-controlled electrochemical behavior of probe DNA at AuNTsA (Li et al., 2012) and obeys the Eqs. (1) and (2)

$$I_a = 1.05 \times 10^{-4} (\text{sqrt of scan rate in mV/s}) + 7.69 \times 10^{-5} (R = 0.9919) \quad (1)$$

$$I_c = -7.18 \times 10^{-5} (\text{sqrt of scan rate in mV/s}) + 1.75 \times 10^{-4} (R = 0.9915) \quad (2)$$

3.3. Selectivity and detection of various concentration of complementary DNA

The DPV measurements were carried out in blank 0.05 M PBS (pH 7.4) for the testing of selectivity and specific hybridization process. Before each measurement, the bioelectrodes were immersed in 20 μM methylene blue (MB) in PBS for 5 min and washed with PBS and the same electrode was used for the measurement. Fig. 5a shows the DPV of probe DNA immobilized AuNTsA (curve i), hybridized complimentary DNA on probe DNA immobilized AuNTsA (curve ii), and non-complementary DNA on probe DNA immobilized AuNTsA (curve iii) electrodes. From the Fig. 5a, it is clearly seems that the probe DNA immobilized electrode has the highest magnitude of the MB peak current (I_p). This may be due to the free guanine bases in probe DNA which has the ability for high accumulation of MB. However, after hybridization of the complementary DNA on probe DNA, the I_p values decreases, indicating the lower MB accumulation on the electrode surfaces during the process of hybridization. After hybridization of the complementary DNA on Probe DNA, there is an unavailability of the free guanine bases and the steric hindrance of the duplex structure may be reason for the decrease of I_p values (Singh et al., 2010). However, there is negligible change in I_p values for non-complementary DNA on the probe DNA electrode observed which is due to the absence of a duplex complex on the electrode surface, indicating the good selectivity of the biosensor.

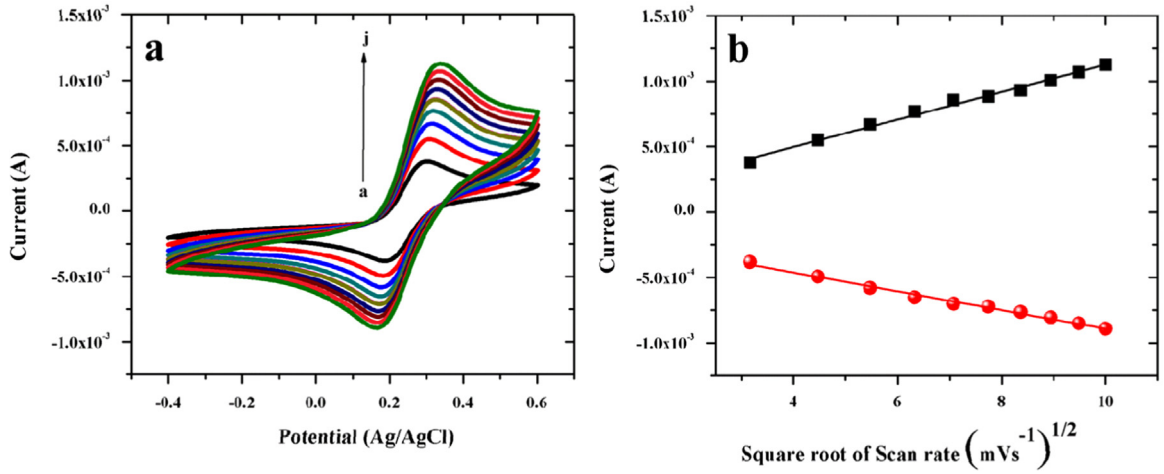

Fig. 4. (a) Cyclic voltagrams of AuNTsA/Probe DNA bioelectrode on increasing scan rate from 10 to 100 mV/s (a–j) in 0.05 m PBS (pH 7.4, 0.15 M NaCl) containing 5 mM $[Fe(CN)_6^{3-/4-}]$ (b) magnitude of current as a function of square root of scan rate (10–100 mV/s).

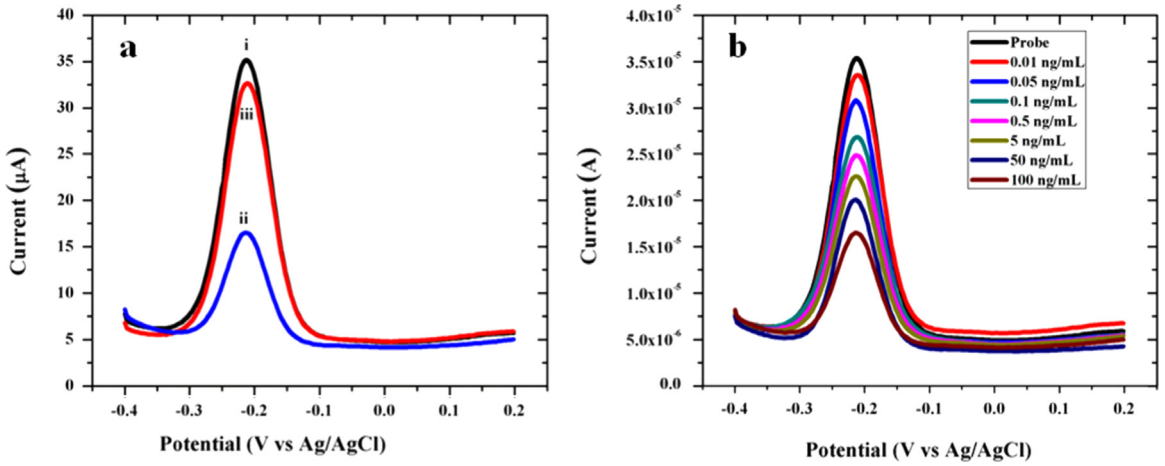

Fig. 5. Differential pulse voltagrams of 20 μM methylene blue in 0.05 M PBS (pH 7.4, 0.15 M NaCl) obtained for (a) (i) AuNTsA/Probe DNA (ii) AuNTsA/Probe /Complementary DNA (iii) AuNTsA/Probe/Non-complementary DNA electrodes (b) AuNTsA/Probe DNA electrode after hybridization with various concentrations of complimentary DNA.

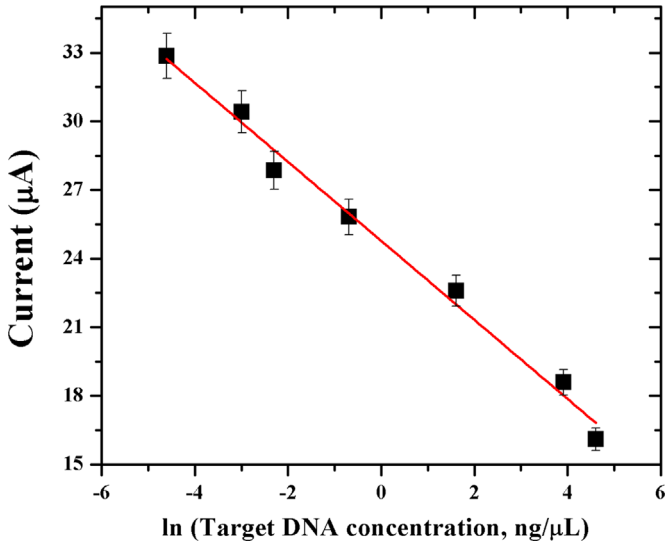

Fig. 6. Linear relationship between the DPV peak current changes with ln (complementary DNA concentration) of AuNTsA/ Probe DNA electrode.

Fig. 5b shows the DPV measurements carried out on probe DNA immobilized AuNTsA electrode upon hybridization with different concentrations ranging from 0.01 ng/μL to 100 ng/μL. As seen from the figure, the I_p values were gradually decreased by increasing the concentration of complementary DNA, indicating that much more duplex structure formation on the electrode surface (Zheng et al., 2014). The I_p values at 0.01 ng/ μL complementary DNA concentrations has been observed to be nearly same as the I_p values of probe DNA, which reveals the absence or negligible of complementary DNA on the electrode surface. Therefore, it may be concluded that 0.05 ng/ μL is detection limit for the AuNTsA electrode. The I_p values vary linearly with different complementary DNA concentration which obeys the following Eq. (3) with regression coefficient 0.987 (Fig. 6).

$$I_a = -1.72 \times 10^{-6} [(\ln \text{ complementary DNA concentration in ng/μL})] + 2.47 \times 10^{-5} \quad (3)$$

3.4. Reproducibility and stability of biosensor

The stability and reproducibility of DNA biosensors are more important to practical applications towards early diagnostics, biomedical and biomedicine. The reproducibility of the AuNTsA and probe DNA immobilized electrode was examined by repeating the CV measurements around 10 cycles and found that there is no significant change in anodic peak and cathodic peak values (data not shown here). When the probe DNA immobilized electrode was stored at 4 °C for around two to three weeks, it retained the significant results of its initial response which indicates the good stability of bioelectrode.

4. Conclusion

The AuNTsA has been synthesized by using electrochemical technique with polycarbonate membrane as the template with 200 nm diameter. The synthesized nanotubes are vertically aligned and strongly attached to the Au thick film and do not affected by the solvent during the etching process of the membrane. The synthesized nanotubes array electrode shows good electrochemical performance than the bare Au electrode. Using this advantage, an electrochemical DNA hybridization biosensor based on the AuNTsA has been fabricated for the detection of *M. tuberculosis* DNA. The developed electrochemical DNA biosensor shows good linear range of complementary DNA concentration from 0.01 ng/ μL to 100 ng/μL with 0.05 ng/μL as the detection limit. The fabricated DNA hybridization sensor will be suitable for the detection of real sample from clinical analytes.

Acknowledgment

This work was supported by NRF (National Research Funds)-Republic of Korea and DST (Department of Science and Technology)-India in the form of India (INT/Korea/P-27)-Korea (NRF-2014K1A3A1A19065626) joint project program.

References

Abdalhai, M.H., Fernandes, A.M., Bashari, M., Ji, J., He, Q., Sun., X., 2014. J. Agric. Food Chem. 62, 12659–12667.
Anandan, V., Rao, Y.L., Zhang, G., 2006. Int. J. Nanomed. 1, 73–79.
Bai, Y., Sun, Y., Sun, C., 2008. Biosens. Bioelectron. 24, 579–585.
Cai, H., Cao, X., Jiang, Y., He, P., Fang, Y., 2003. Anal. Bioanal. Chem. 375, 287–293.
Chang, H., Yuan, Y., Shi, N., Guan, Y., 2007. Anal. Chem. 79, 5111–5115.
Chavolla, E.T., Alocilja, E.C., 2011. Biosens. Bioelectron. 26, 4614–4618.
Chiti, G., Marrazza, G., Mascini, M., 2001. Anal. Chim. Acta 427, 155–164.
Das, M., Sumana, G., Nagarajan, R., Malhotra, B.D., 2010. Appl. Phys. Lett. 96, 133703.
Devi, R.V., Doble, M., Verma, S.R., 2015. Biosens. Bioelectron. 68, 688–698.

Du, P., Li, H., Mei, Z., Liu, S., 2009. Bioelectrochemistry 75, 37–43.
Fan, J.G., Dyer, D., Zhang, G., Zhao, Y.P., 2004. Nano Lett. 4, 2132–2138.
Fu, Y., Yuan, R., Xu, L., Chai, Y., Liu, Y., Tang, D., Zhang, Y., 2005. J. Biochem. Biophys. Methods 62, 163–174.
Gasparac, R., Taft, B.J., Devlin, M.A.L., Lazareck, A.D., Xu, J.M., Kelley, S.O., 2004. J. Am. Chem. Soc. 126, 12270–12271.
Hill, H.D., Millstone, J.E., Banholzer, M.J., Mirkin, C.A., 2009. ACS Nano 3, 418–424.
Hong, S.W., Banks, T., Rogers, J.A., 2010. Adv. Mater. 22, 1826–1830.
Hrdy, R., Kynclova, H., Drbohlavova, J., Svatos, V., Chomoucka, J., Prasek, J., Businova, P., Pekarek, J., Trnkova, L., Kizek, R., Hubalek, J., 2013. Int. J. Electrochem. Sci. 8, 4384–4396.
Kara, P., Cavusoglu, C., Cavdar, S., Ozsoz, M., 2009. Biosens. Bioelectron. 24, 1796–1800.
Kralchevsky, P.A., Nagayama, K., 2000. Adv. Colloid Interface Sci. 85, 145–192.
Lee, H.E., Kang, Y.O., Choi, S.H., 2014. Int. J. Electrochem. Sci. 9, 6793–6808.
Lee, S.J., Anandan, V., Zhang, G., 2008. Biosens. Bioelectron. 23, 1117–1124.
Lei, B.X., Luo, Q.P., Sun, Z.F., Kuang, D.B., Su, C.Y., 2013. Adv. Powder Technol. 24, 175–182.
Li, W., Wang, X., Chen, X., Liu, J., Liu, S., Zhao, C., 2012. Bioelectrochemistry 88, 30–35.
Li, F., Han, X., Liu, S., 2011. Biosens. Bioelectron. 26, 2619–2625.
Lin, C.C., Juo, T.J., Chen, Y.J., Chiou, C.H., Wang, H.W., Liu, Y.L., 2008. Desalination 233, 113–119.
Lin, Y., Fang Lu, F., Tu, Y., Ren, Z., 2004. Nano Let. 4, 191–195.
Lu, L.M., Zhang, L., Qu, F.L., Lu, H.X., Zhang, X.B., Wu, Z.S., Huan, S.Y., Wang, Q.A., Shen, G.L., Yu, R.Q., 2009. Biosens. Bioelectron. 25, 218–223.
Naderi, N., Hashim, M.R., Rouhi, J., 2012. Int. J. Electrochem. Sci. 7, 8481–8486.
Prabhakar, N., Arora, K., Arya, S.K., Solanki, P.R., Iwamoto, M., Singh, H., Malhotra, B. D., 2008. Analyst 133, 1587–1592.
Ramulu, T.S., Venu, R., Sinha, B., Lim, B., Jeon, S.J., Yoon, S.S., Kim, C.G., 2013. Biosens. Bioelectron. 40, 258–264.
Singh, R., Sumanna, G., Verma, R., Sood, S., Pandey, M.K., Gupta, R.K., Malhotra, B.D., 2010. J. Biotechnol. 150, 357–365.
Shukla, R., Bansal, V., Chaudhary, M., Basu, A., Bhonde, R.R., Sastry, M., 2005. Langmuir 21, 10644–10654.
Soundararajan, D., Yoon, J.K., Kim, Y.I., Kwon, J.S., Park, C.W., Kim, S.H., Ko, J.M., 2009. Int. J. Electrochem. Sci. 4, 1628–1637.
Szunerits, S., Coffinier, Y., Boukherroub, R., 2015. Sensors 15, 12573–12593.
Tang, Y.B., Bo, X.H., Lee, C.S., Cong, H.T., Cheng, H.M., Chen, Z.H., Zhang, W.J., Bello, I., Lee, S.T., 2008. Adv. Funct. Mater. 18, 3515–3522.
Wang, C., Yang, C., Song, Y., Gao, W., Xia, X., 2005. Adv. Funct. Mater. 15, 1267–1275.
Wang, H., Wang, X., Zhang, X., Qin, X., Zhao, Z., Miao, Z., Huang, N., Chen, Q., 2009. Biosens. Bioelectron. 25, 142–146.
Wang, W., Fan, X., Xu, S., Davis, J.J., Luo, X., 2015. Biosens. Bioelectron. 71, 51–56.
Wang, Y., Zhu, Y., Chen, J., Zeng, Y., 2012. Nanoscale 4, 6025–6031.
WHO Global Tuberculosis Report, 2014. ⟨http://www.who.int/tb/publications/global_report/en/⟩.
Yang, G., Li, L., Jiang, J., Yang, Y., 2012. Mater. Sci. Eng. C 32, 1323–1330.
Yang, M., Qu, F., Lu, Y., He, Y., Shen, G., Yu, R., 2006. Biomaterials 27, 5944–5950.
Yang, X., Yuan, L., Peterson, V.K., Yin, Y., Minett, A.I., Harris, A.T., 2011. J. Phys. Chem. C 115, 14093–14097.
Yuzvinsky, T.D., Fennimore, A.M., Kis, A., Zettl, A., 2006. Nanotechnology 17, 434–438.
Zheng, D., Wang, Q., Gao, F., Wang, Q., Qiu, W., Gao, F., 2014. Biosens. Bioelectron. 60, 167–174.